Available online at www.sciencedirect.com

SCIENCE @ DIRECT®

ELSEVIER

Journal of Nuclear Materials 325 (2004) 13–17

journal of nuclear materials

www.elsevier.com/locate/jnucmat

Corrosion behavior of Fe–Ni–Cr alloys in the molten salt of LiCl–Li_2O at high temperature

S.H. Cho [a,*], J.S. Zhang [b], Y.J. Shin [a], S.W. Park [a], H.S. Park [a]

[a] Korea Atomic Energy Research Institute, 150 Duckjindong, Yusong-Ku, Taejon 305-353, South Korea
[b] Department of Materials Engineering, Dalian University of technology, Dalian 116023, China

Received 18 June 2001; accepted 16 October 2003

Abstract

At Korea Atomic Energy Research Institute (KAERI), we investigated the corrosion behavior of a series of Fe–Cr–Ni alloys with different chromium contents in molten LiCl and molten LiCl–25wt%Li_2O mixture at temperatures ranging from 923 to 1123 K. In molten LiCl, dense protective scale of $LiCrO_2$ grows outwardly while corrosion is accelerated by addition of Li_2O to LiCl. The basic fluxing of Cr_2O_3 by Li_2O would be the cause of accelerated corrosion. Because of low oxygen solubility and very high Li_2O activity in the molten LiCl–Li_2O mixture, Cr is preferentially corroded while Ni remains stable and thus, corrosion rate of the alloys in molten LiCl–Li_2O mixture increases with an increase in Cr content.

PACS: 82.45.Bb

1. Introduction

Corrosion of alloys in molten salts has been studied extensively. The accelerated oxidation of the Ni-base Superalloys (Hot Corrosion) is one of the important fields of the corrosion. The presence of a film of molten Na_2SO_4 deposit is the cause of the accelerated oxidation [1–6]. The more the basicity (activity of Na_2O) of the molten salt increases, the more Na_2O reacts with the protective NiO scale that was formed on the surface of the alloy and produces NiO_2^{2-}, and the NiO_2^{2-} dissolves into the molten salt. As the protective oxide scale is removed, the corrosion of the alloy rapidly takes place. This mechanism is called basic fluxing of the protective oxide scale [4–6]. During the corrosion process, a porous oxide scale is formed by the re-precipitation of NiO in the molten salt. The re-precipitation takes place due to the negative gradient of salt basicity in the salt film [4–6]. Although Cr_2O_3 has high solubility in molten basic Na_2SO_4 [7,8], in general, a high concentration of Cr can prevent the accelerated oxidation of the alloy. This is because, in the presence of Cr_2O_3, it reacts with the Na_2O and reduces its activity in the molten salt and prevents further dissolution of the protective NiO scale [5].

The Korea Atomic Energy Research Institute has investigated a new approach for the spent fuel storage technology. The technology utilizes the reduction of oxide fuel to a metal for the reduction of the total storage volume and preferentially removing the fission products to reduce the decay heat. The uranium oxide is reduced to metallic uranium by Li metal in a molten LiCl bath. The Li_2O that formed during the reduction process is soluble in the bath. Previously we have investigated the corrosion behavior of some commercial alloys in LiCl–Li_2O molten salts [9–11]. Because Li_2O is a strong basic oxide, its corrosion behavior for alloys in a molten LiCl–Li_2O mixture is considered to be similar

---

[*] Corresponding author. Tel.: +82-42 868 2584; fax: +82-42 868 8370.
E-mail address: nshcho1@kaeri.re.kr (S.H. Cho).

0022-3115/$ - see front matter © 2003 Elsevier B.V. All rights reserved.
doi:10.1016/j.jnucmat.2003.10.011

to that of the Na_2O in molten Na_2SO_4. It has been observed that corrosion is significantly accelerated by the addition of 25 wt% Li_2O to LiCl, and also that a porous oxide scale grows inwardly at the alloy/scale interface. However, the corrosion product is $LiCrO_2$, not the expected Cr_2O_3 or NiO in the salt bath of 25 wt% Li_2O, and the high Cr content in the alloys did not reduce the corrosion process. Furthermore, in case of all the commercial alloys that have been investigated, such as stainless steel 304L, 316L [9], heat resistant cast steel More l and Super 22H [10], Ni-base Superalloys Inconel 600, and Hastelloy C-276 [11], the corrosion of these alloys follows the linear rate law. In the present study, we investigated the corrosion behavior of a series of Fe–Ni–Cr alloys with different Cr content in molten salt of LiCl and LiCl–25%Li_2O mixture at the temperature range of 923–1123 K. The main purpose of this study is to clarify the effect of Cr content on corrosion in a molten LiCl–25%Li_2O mixture and, thereby, obtain the data necessary for designing corrosion resistant alloys in molten LiCl–Li_2O systems.

2. Experimental

The chemical compositions of the alloys studied are presented in Table 1. These Fe-base alloys have similar Ni contents with varying amounts of Cr. First the test samples of KSA (Kaeri SuperAlloy)-4 and KSA-5 alloys were melted in a vacuum induction furnace. The ingots were hot-rolled to a plate of 17 mm thick and annealed at 1323 K for 1 h. Incoloy 800H is the alloy commercially available by HPA (High Performance Alloys, Inc.). High purity reagent of LiCl and Li_2O were used. Impurity contents are $Na < 0.2\%$, $Ca < 0.05\%$, $Fe < 0.001\%$, $SO_4 < 0.05\%$ and $H_2O < 0.43\%$ for LiCl and $Ca < 0.01\%$, $Fe < 0.01\%$, $Si < 0.01\%$ for Li_2O.

All the samples were made into test specimens with a size of $15 \times 20 \times 2.5$ mm^3, ground with grade 800 SiC paper, and ultrasonically degreased in acetone. These specimens were immersed in a crucible of 22 g of LiCl and/or LiCl–25wt%Li_2O mixture at temperatures ranging from 923 to 1123 K. The corrosion products were removed by ultrasonically cleansing the specimens in 10% HNO_3. The weight losses of the specimens after the cleansing would be the total amount of corrosion in a given time.

Some corroded specimens were investigated by X-ray diffraction (XRD), scanning electron microscopy (SEM) and electron probe microanalysis.

3. Results

Fig. 1 shows the amount of weight loss for the alloys. The corrosion experiments were conducted in molten baths of LiCl and LiCl–25%Li_2O mixture at 923, 1023 and 1123 K for 25 h. It is seen from the figure that: (1) the corrosion rates of the alloys in molten LiCl are relatively low and little distinction between the alloys is observed, (2) corrosion of the alloys is significantly accelerated by addition of Li_2O to LiCl and the rate of acceleration is higher with increase in temperature, (3) corrosion rate increases with higher Cr content for the alloy in molten LiCl–25%Li_2O mixture.

The time dependency of the metal losses at 1023 K is shown in Fig. 2. The lines in the figure are theoretical curves for linear and parabolic rate law, respectively. Corrosion rates of the alloys in molten LiCl decrease rapidly with time, following parabolic rate law. How-

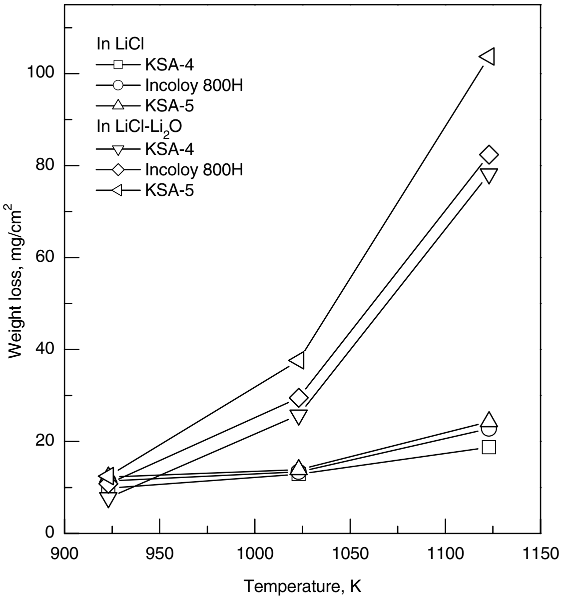

Fig. 1. Weight losses of the alloys corroded in molten LiCl and LiCl–25%Li_2O mixture for 25 h, as a function of temperature.

Table 1
Chemical composition of the tested alloys (wt%)

Alloys	C	Cr	Ni	Si	Mn	S	P	Fe
KSA-4	<0.03	8.0	36.0	<0.5	<0.5	<0.03	<0.03	bal.
Incoloy 800H	0.08	22.0	31.0	0.53	1.07	0.006	0.006	bal.
KSA-5	<0.03	29.0	32.0	<0.5	<0.5	<0.03	<0.03	bal.

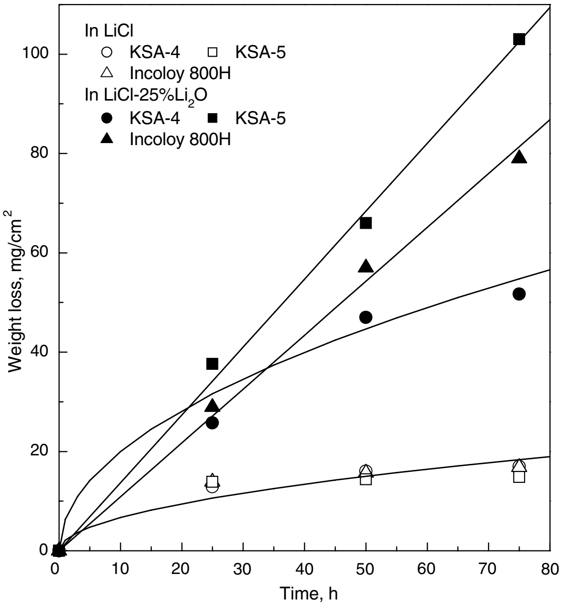

Fig. 2. Weight losses of the alloys corroded in molten LiCl and LiCl–25%Li_2O mixture at 1023 K, as a function of time.

ever, in the molten LiCl–25wt%Li_2O mixture, the corrosion of alloys containing a high Cr content (KSA-5 and Incoloy 800H) follow the linear rate law, while for the alloy with a low Cr content (KSA-4), the linear rate law breaks down after 25 h and then the corrosion rate decreases with time. So corrosion kinetics of KSA-4 in the molten mixture cannot be describe simply as linear or parabolic.

We see that a dense protective scale of $LiCrO_2$ was formed, as seen from the SEM microstructure (Fig. 3) and X-ray diffraction patterns (Fig. 4) of the scales that formed on the surface of the alloys in molten LiCl. In the molten LiCl–25%Li_2O mixture, through SEM (Fig. 5) observation and X-ray diffraction (Fig. 6), we see that the scales on the alloys containing a high Cr content (Incoloy 800H and KSA-5) are porous and consist of two phases: a dark matrix and light islands (Fig. 5(a)).

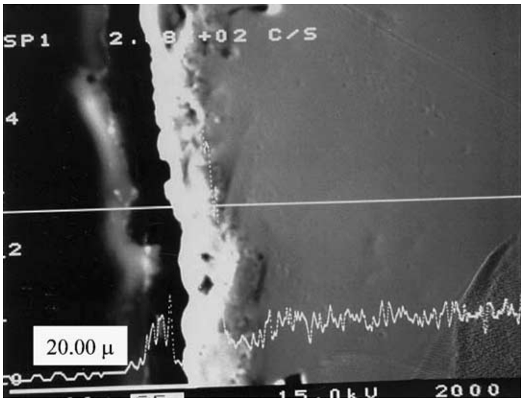

Fig. 3. Microstructure and line scan X-ray analysis showing Cr concentrated in the scale on KSA-4 alloy corroded in molten LiCl at 1023 K for 25 h.

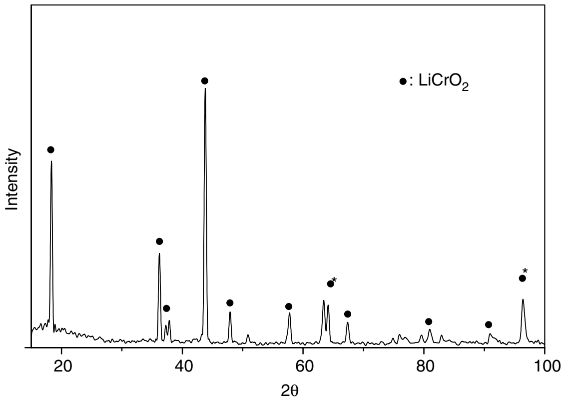

Fig. 4. X-ray diffraction patterns from the scale on KSA-4 alloy corroded in molten LiCl at 1023 K for 25 h.

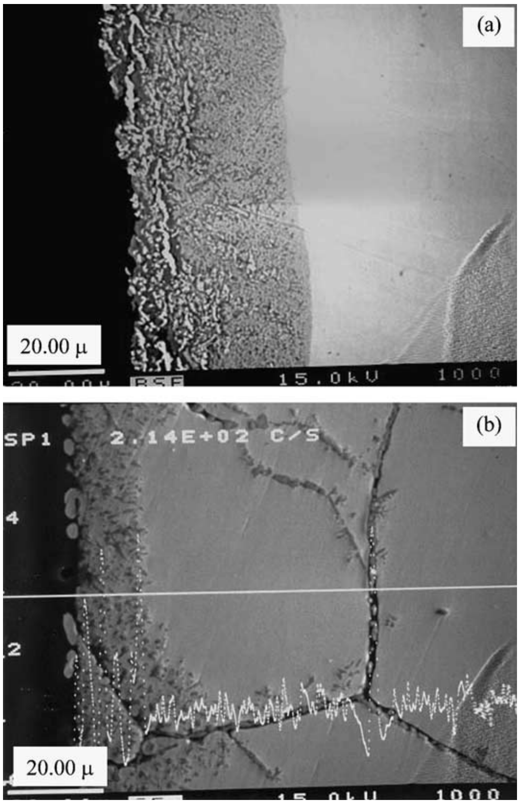

Fig. 5. Microstructures of the scales on Incoloy 800H (a) and KSA-4 alloy (b) corroded in molten LiCl–25%Li_2O mixture at 1023 K for 25 h.

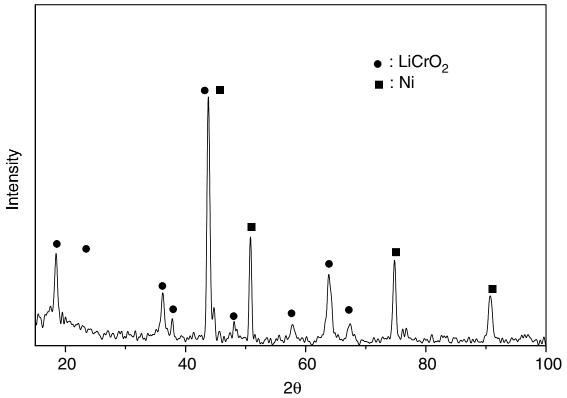

Fig. 6. X-ray diffraction patterns from the scale on Incoloy 800H corroded in molten LiCl–25%Li_2O at 1023 K for 25 h.

These two phases are identified to be $LiCrO_2$ (dark phase) and Ni-rich solid solution (light islands). However, for the KSA-4 alloy of low Cr content, Cr-rich oxide particles are distributed at the grain boundaries and under the surface, indicating the typical feature of internal corrosion (Fig. 5(b)). Because the amount of the particles is small (XRD is not available) and Li is a light element (EPMA is not available), type of the oxide of Cr_2O_3 or $LiCrO_2$ is not expected and we have not identified them. Further work is needed for detailed studies.

4. Discussion

Corrosion in molten salts is characterized by two steps. The first is oxidation of metal and the second is basic or acidic dissolution of the oxide [12,13]. In the present case of molten LiCl the first step can be expressed as

$$2Cr + 3/2O_2 = Cr_2O_3 \tag{1}$$

For the second step, basic dissolution of Cr_2O_3 cannot take place because the basic oxide Li_2O do not exist in the melt, and so the formation of $LiCrO_2$ can be expressed as

$$Cr_2O_3 + 2LiCl + 1/2O_2 = 2LiCrO_2 + Cl_2 \tag{2}$$

The impurity water in LiCl may play the same role as O_2 and, therefore, accelerates the corrosion rate to some extent.

Because Cr_2O_3 scale is usually dense protective, the $LiCrO_2$ scale that formed directly from the Cr_2O_3 scale is also dense protective. According to Wagner's theory [14] corrosion rate in this case would be controlled by diffusion of Cr from substrate to scale/melt interface and, therefore, the corrosion would exhibit parabolic kinetics. This is in agreement with the kinetics in Fig. 2 in which corrosion in molten LiCl shows approximate parabolic rate law.

As for oxidant O_2 in the reactions, Indacochea and Smith found that the oxygen dissolved into molten LiCl from gas phase acts as important role, and that when the corrosion test in molten LiCl was carried out in an argon atmosphere, the sample was not suffered from corrosion attack [15].

When Li_2O is added to LiCl, we observed the alloys change the corrosion rate, reaction kinetics, and structure of the scale. Because Li_2O is a strong basic oxide, the Li_2O is expected to act as the basic fluxing agent to Cr_2O_3 on the corrosion behavior of alloys. That is, after the first step of Cr_2O_3 formation (reaction (1)), Li_2O reacts with Cr_2O_3 and form chromate ions that dissolve into the molten salt

$$Cr_2O_3 + 3/2O_2 + 2Li_2O = 2Li_2CrO_4 \tag{3}$$

Since the protective scale of Cr_2O_3 is removed by reaction (3) the corrosion proceeds rapidly. Corrosion process above-mentioned is similar to the case of hot corrosion caused by the film of molten Na_2SO_4 deposit [1,4,5], that is the basic fluxing of protective scale by the basic oxide Na_2O. In the present case, however, Cr_2O_3 re-precipitation would not take place in the molten mixture because the gradient of activities of both the basic oxide Li_2O and oxygen in the vicinity of the alloy/salt interface is positive. That is, at the interface, activities of both the Li_2O and oxygen decrease due to reactions (1) and (3) while activities of both the Li_2O and oxygen remain original values in the molten mixture away from the interface. According to the phase stability diagram of Na–Cr–S–O presented by Rapp [7], the chromate ions (CrO_4^{2-}) stay stable in molten Na_2SO_4 with relatively high activity of basic oxide Na_2O and/or oxygen while the chromate ions (CrO_4^{2-}) is reduced to CrO_2^- (solid $NaCrO_2$) when the activity of Na_2O and/or oxygen decrease. Similarly, in the present case, when the concentration of oxygen and/or Li_2O at the alloy/salt interface decreases, to a certain level due to reactions (1) and (3), the Li_2CrO_4 would be reduced to $LiCrO_2$ and precipitate on the surface of the sample to form porous non-protective scale, as

$$Li_2CrO_4 = LiCrO_2 + 3/4O_2 + 1/2Li_2O \tag{4}$$

If the oxidation rate of Cr (reaction (1)) were faster than the fluxing rate of Cr_2O_3 (reaction (3)), a dense protective Cr_2O_3 scale would form at the surface of the alloy. The formation of the porous $LiCrO_2$ scale indicates that reaction (1) is a slower step of the sequential processes of reactions (1) and (3) and, therefore, the corrosion rate is determined by reaction (1). It is thus concluded that the higher the Cr content in an alloy, the faster the rate of reaction (1) is, and also the higher the corrosion rate of the alloy would be.

In the molten LiCl–25%Li_2O mixture, the concentration of Li_2O is so high and the amount of the molten mixture is so large (22 g) that the decrease in the basicity (activity of Li_2O) of the molten salt caused by the corrosion reactions would be negligible. Therefore, a high Cr content in an alloy could not improve the corrosion resistance of the alloy. However, solubilities of oxygen in several molten salts, such as sulfate and carbonate melts, were determined to be very low [16]. So oxygen activity in the present case of molten LiCl–Li_2O is also expected to be low and, therefore, Cr is preferentially oxidized and Ni remains stable in the molten mixture. When the Cr-rich corrosion product grows inwardly, Ni-rich island is formed and finally forms the scale, producing a two-phase structure of the scale.

The internal corrosion observed in KSA-4 alloy (Fig. 5(b)) is related to a low Cr content in the alloy and the selective oxidation of Cr in the molten mixture. It should be noted, however, that internal corrosion did not occur in molten LiCl, indicating that Li_2O play an important role in the internal corrosion process. In order to understand the mechanism of internal corrosion and the complex kinetics observed in KSA-4 alloy, further work is needed.

The details of the behavior of Fe during the corrosion process were not well understood in the current studies. Fe-rich corrosion products were not detected in the corroded specimens in current and in earlier studies [6–8], though Fe is always detected in the salt after the corrosion tests. For example, content of Fe, Cr, Ni in the LiCl–25%Li_2O mixture after the corrosion test of Incoloy 800H at 1123 K for 25 h is 1.15, 0.01 and 0.12 wt% respectively. This implies that Fe in the alloys is dissolved into the molten mixture by some unknown mechanisms.

5. Conclusions

The corrosion behavior of a series of Fe–Ni–Cr alloys with different Cr content were investigated in molten LiCl and LiCl–25%Li_2O mixture at high temperatures. The effects of Cr content in the alloys were discussed. The results obtained are summarized as follows:

(1) In molten LiCl, a dense protective scale of $LiCrO_2$ grows outwardly and the alloys containing Cr content higher than 8% provide good resistance to the corrosion.
(2) When Li_2O is added to the molten salt, corrosion of the alloys is accelerated and the effect of Li_2O is the basic fluxing of the protective scale of Cr_2O_3 by basic oxide Li_2O.
(3) In the molten LiCl–25%Li_2O mixture, a porous scale consisting of $LiCrO_2$ and Ni-rich solid solution is formed on the surface of alloys containing high Cr content and the internal corrosion occurs in the alloy with low Cr content.
(4) Corrosion rate of the Fe–Cr–Ni alloy in the molten LiCl–25%Li_2O mixture increases with the increasing Cr content in the alloys.

Acknowledgements

This study has been carried out under the Nuclear R&D Program supported by Ministry of Science and Technology of Korea.

References

[1] W.T. Reid, R.C. Corey, B.J. Cross, Trans. ASME 67 (1945) 279.
[2] N.S. Bornstein, M.A. DeCrescente, Trans. Met. Soc. AIME 245 (1969) 583.
[3] N.S. Bornstein, M.A. DeCrescente, Met. Trans. 2 (1971) 2875.
[4] J.A. Goebel, F.S. Pettit, Met. Trans. 1 (1970) 1943.
[5] J.A. Goebel, F.S. Pettit, G.W. Goward, Met. Trans. 4 (1973) 261.
[6] R.A. Rapp, Y.S. Zhang, Molten Salt Forum. 5&6 (1998) 25.
[7] R.A. Rapp, Mater. Sci. Eng. 87 (1987) 319.
[8] Y.S. Zhang, J. Electrochem. Soc. 133 (1986) 655.
[9] S.H. Cho, S.C. Park, M.S. Jeong, J.S. Zhang, Y.J. Shin, Korean J. Mater. Res. 9 (1999) 211.
[10] S.H. Cho, S.C. Park, J.S. Zhang, Y.J. Shin, H.S. Park, Korean J. Mater. Res. 9 (1999) 556.
[11] S.H. Cho, J.S. Zhang, M.S. Jeong, S.C. Oh, Y.J. Shin, Korean J. Mater. Res. 9 (1999) 985.
[12] N. Birks, G.H. Maier, Introduction to High Temperature Oxidation of Metals, Adward Arnold, London, 1979.
[13] M. Spiegel, P. Biedenkopf, J. Grabke, Corros. Sci. 39 (1997) 1193.
[14] C. Wagner, Z. Phys. Chem. (B) 21 (1933) 25.
[15] J.E. Indacochea, J.L. Smith, J. Mater. Res. 14 (1999) 1990.
[16] R.E. Andresen, J. Electochem. Soc. 126 (1979) 328.